J|A|C|S
ARTICLES
Published on Web 06/12/2004

Hydration of Alumina Cluster Anions in the Gas Phase

Anita K. Gianotto,[†] Jennifer W. Rawlinson,[‡] Kevin C. Cossel,[†] John E. Olson,[†] Anthony D. Appelhans,[†] and Gary S. Groenewold*,[†]

Contribution from the Idaho National Engineering and Environmental Laboratory, Idaho Falls, Idaho 83415, and Brigham Young University-Idaho, Rexburg, Idaho 83460

Received February 9, 2004; E-mail: gsg@inel.gov

Abstract: Hydration reactions of anionic aluminum oxide clusters were measured using a quadrupole ion trap secondary ion mass spectrometer, wherein the number of Lewis acid sites were determined. The extent of hydration varied irregularly as cluster size increased and indicated that the clusters possessed condensed structures where the majority of the Al atoms were fully coordinated, with a limited number of undercoordinated sites susceptible to hydrolysis. For maximally hydrated ions, the number of OH groups per Al decreased in an exponential fashion from 4.0 in Al_1 cluster to 1.4 in the Al_9 cluster, which was greater than that expected for a highly hydroxylated surface but less than that for solution phase alumina clusters.

Introduction

The structure and accompanying reactivity of aluminum oxide has tremendous importance in a broad range of processes. Alumina is used extensively as a catalyst and as a catalyst support,[1,2] and in fact "dislodged" alumina may be responsible for some of the catalytic activity of zeolites.[3−5] Alumina is present as a 10−20 Å film on aluminum metal surfaces, where it exerts a strong influence on manufacturing processes.[6] In the environment,[7] it functions as an adsorbent and as a toxin,[8] and flocculated alumina has recently been shown to inactivate viruses.[9] In the atmosphere, aluminum oxide clusters are generated from space shuttle launches and may play a role in atmospheric reactions.[10−14]

The chemical properties of alumina are a strong function of its explicit molecular speciation at the molecular level, both on the surfaces of bulk materials, and on small clusters. In particular, undercoordinated Al atoms function as Lewis acids and surface hydroxyls as Bronsted acids, which, when deprotonated form reactive conjugate bases. These functional groups directly control a myriad of processes and are intimately related to one another by hydrolysis and dehydroxylation reactions. The undercoordinated Al sites arise in part from the thermodynamic need that alumina surfaces have to minimize surface free energy, which they accomplish by relaxing Al atoms away from the surface;[15−19] this movement is thought to produce sp^2 hybridized aluminum atoms capable of strong Lewis acid behavior.[20] Hydrolysis reactions at these sites produce hydroxyl groups that have also been shown to induce surface relaxation[21,22] and are key to metal island growth on catalyst materials.[2,23−25] Undercoordinated Lewis acid sites can be reformed by dehydration from adjacent OH groups.[1,3,8,24,26,27]

These phenomena motivated surface investigations of both the surface Al atoms and the OH moieties. X-ray photoelectron spectroscopy was used to measure hydroxyl surface density,[28]

[†] Idaho National Engineering and Environmental Laboratory.
[‡] Brigham Young University−Idaho.

(1) Knozinger, H.; Ratnasamy, P. *Catal. Rev.—Sci. Eng.* **1978**, *17*, 31−70.
(2) Ertl, G.; Freund, H.-J. *Phys. Today* **1999**, 32−38.
(3) Coster, D.; Blumenfield, A. L.; Fripiat, J. J. *J. Phys. Chem.* **1994**, *98*, 6201−6211.
(4) Sanz, J.; Fornes, V.; Corma, A. *J. Chem. Soc., Faraday Trans. 1* **1988**, *84*, 3113−3119.
(5) Pellet, R. J.; Blackwell, C. S.; Rabo, J. A. *J. Catal.* **1988**, *114*.
(6) Sercombe, T. B.; Schaffer, G. B. *Science* **2003**, *301*, 1225−1227.
(7) Brown, G. E. J.; Henrich, V. E.; Casey, W. H.; Clark, D. L.; Eggleston, C.; Felmy, A.; Goodman, D. W.; Gratzel, M.; Maciel, G.; McCarthy, M. I.; Nealson, K. H.; Sverjensky, D. A.; Toney, M. F.; Zachara, J. M. *Chem. Rev.* **1999**, *99*, 77−174.
(8) Evans, L. J. *Environ. Sci. Technol.* **1989**, *23*, 1046−1056.
(9) Matsui, Y.; Matsushita, T.; Sakuma, S.; Gojo, T.; Mamiya, T.; Suzuoki, H.; Inoue, T. *Environ. Sci. Technol.* **2003**, *37*, 5175−5180.
(10) Cofer, W. R., III; Lala, G. G.; Wightman, J. P. *Atmos. Environ.* **1987**, *21*, 1187−1196.
(11) Laredo, D.; McCrorie, J. D., II; Vaughn, J. K.; Netzer, D. W. *J. Propul. Power* **1994**, *10*, 410−418.
(12) Dill, K. M.; Reed, R. A.; Calia, V. S.; Schulz, R. J. *J. Propul. Power* **1990**, 668−671.
(13) Prather, M. J.; Garcia, M. M.; Douglass, A. R.; Jackman, C. H.; Ko, M. K. W.; Sze, N. D. *J. Geophys. Res.* **1990**, *95*, 18583−18590.
(14) Potter, A. E. *J. Environ. Sci.* **1978**, 15−21.
(15) Guenard, P.; Renaud, G.; Barbier, A.; Gautier-Soyer, M. *Surf. Rev. Lett.* **1997**, *5*, 321−324.
(16) Causa, M.; Dovesi, R.; Roetti, C.; Kotomin, E.; Saunders, V. R. *Chem. Phys. Lett.* **1987**, *140*, 120−123.
(17) Manassidis, I.; De Vita, A.; Gillan, M. J. *Surf. Sci. Lett.* **1993**, *285*, L517−L521.
(18) Pisani, C.; Causa, M.; Dovesi, R.; Roetti, C. *Prog. Surf. Sci.* **1987**, *254*, 119−137.
(19) Puchin, V. E.; Gale, J. D.; Shluger, A. L.; Kotomin, E. A.; Gunster, J.; Brause, M.; Kempter, V. *Surf. Sci.* **1997**, *370*, 190−200.
(20) Godin, T. J.; Lafemina, J. P. *Phys. Rev. B.* **1994**, *49*, 7691−7696.
(21) McHale, J. M.; Auroux, A.; Perrotta, A. J.; Navrotsky, A. *Science* **1997**, *277*, 788−791.
(22) Eng, P. J.; Trainor, T. P.; Brown, J. G. E.; Waychunas, G. A.; Newville, M.; Sutton, S. R.; Rivers, M. L. *Science* **2000**, *288*, 1029−1033.
(23) Heemeier, M.; Frank, M.; Libuda, J.; Wolter, K.; Kuhlenbeck, H.; Baumer, M.; Freund, H.-J. *Catal. Lett.* **2000**, *68*, 19−24.
(24) Libuda, J.; Frank, M.; Sandell, A.; Andersson, S.; Bruhwiler, P. A.; Baumer, M.; Martensson, N.; Freund, H.-J. *Surf. Sci.* **1997**, *384*, 106−119.
(25) Chambers, S. A.; Droubay, T.; Jennison, D. R.; Mattsson, T. R. *Science* **2002**, *297*, 827−831.
(26) Fitzgerald, J. J.; Piedra, G.; Dec, S. F.; Seger, M.; Maciel, G. E. *J. Am. Chem. Soc.* **1997**, *119*, 7832−7842.
(27) Chen, F. R.; Davis, J. G.; Fripiat, J. J. *J. Catal.* **1992**, *133*, 263−278.
(28) McCafferty, E.; Wightman, J. P. *Surf. Interface Anal.* **1998**, *26*, 549−564.

and diffuse reflectance FTIR indicated substantial reconstruction of α-Al_2O_3 surfaces upon exposure to H_2O, resulting in Al-$(OH)_3$ phases.[29] Synchrotron spectroscopic methods helped elucidate surface relaxation[15,22] and provided additional information on hydrated alumina surfaces.[22] However, using bulk materials, it is difficult to directly examine the reactivity of alumina materials. One intriguing approach was to utilize isotopic oxygen exchange of aqueous Al_{13} oxide complexes, which were probed using NMR spectroscopy.[30,31] Under ambient conditions, rate of ^{17}O-for-^{16}O exchange varied significantly depending on whether the O was present as adsorbed molecular water, a HO^- ligand, or an oxo moiety.

On account of experimental challenges associated with the alumina systems, many in the research community have turned to computational chemistry to examine alumina structure and reactivity. These studies have emphasized clusters because they are computationally more easily handled than are surfaces. A triangular structure was calculated for AlO_2,[32] but once clusters exceed this size, the structures tend to contain rhomboid rings. This tendency generally holds for ionic and neutral Al_2O_2,[33,34] Al_2O_3,[34−36] and Al_2O_4,[33,37] although only linear structures have been definitely observed for Al_2O_x ($x = 2, 3, 4$) in matrix isolation studies. The rhombic structural theme was also prominent in calculations of Al_3O_y systems, although there are two competitive variations, viz., a rhombus with pendant atoms and a bent "windowpane" structure (which can be viewed as two "fused" rhombuses) having C_{2v} symmetry. The two variations were competitive for $y = 3$,[38−40] and similar results were obtained for $y = 4$[41] and $y = 5$.[42] For Al_4O_4, a planar D_{2h} rhombus structure with two −O−Al moieties attached to the Al corners was most stable; however, a cubic T_d structure was calculated to be within a few kcal mol^{-1} in energy.[43]

Experimentally, investigations of alumina clusters have not been extensive, probably because it is hard to get large highly oxidized metals into the gas phase. Initial experiments showed that large, unoxidized Al_n cluster neutrals and ions could be generated using either keV Ar impact[44,45] or laser ablation,[46−48] which enabled studies of mobility[46] and reactivity. However, exposure of the metal clusters to O_2 resulted in oxidative dissociation[44,45,49−51] and did not form more oxidized species that would be characteristic of an alumina surface.

Laser ablation also produced more highly oxidized $Al_3O_n^-$ ($1 \le n \le 5$), which enabled measurement of their photoelectron spectra[52] and indicated the presence of multiple isomers for $1 \le n \le 4$, in agreement with the computational studies.[40] The lowest energy structures all contained rhombic moieties, but for $Al_3O_3^-$, a hexagonal structure was within 15 kcal mol^{-1}. Fast neutral bombardment[53] of Al oxides and bare metal produced cationic $Al_xO_y^+$ that tended to undergo oxidation until all Al centers were trigonally coordinated.[47] MNDO calculations conducted as part of that study indicated, for $Al_2O_4^+$ and $Al_3O_6^+$, structures containing four- and six-membered rings were preferred (respectively), consistent with the above-cited studies.

Solvation studies were employed as a means to probe the structure of gaseous $Al_3O_3^-$, which reacted with H_2O and methanol producing stable $Al_3O_3^-(solvent)_{1,2}$.[54] It was suggested that both solvent molecules were added to the central, trigonally coordinated Al of the windowpane structure.[39] Interestingly, under what were termed saturated conditions, doubly and triply hydrated $Al_2O_4H^-$ and $Al_3O_6H_2^-$ were observed. This result is identical to that reported previously by our group for $Al_2O_4H^-$, which rapidly added one and two H_2O molecules.[55] This research also showed that AlO_2^- would add two H_2O molecules forming $Al(OH)_4^-$, but at a much slower rate than would the Al_2 species. Hartree−Fock and density functional theory (DFT) calculations performed as part of Scott's study[55] showed that although the initial water adducts were hydrogen-bound, hydrolysis occurred by nucleophilic attack of the H-bound H_2O on the trigonal Lewis acid sites on the anions, indicating that H_2O could be used as a derivatizing agent for the reactive Al centers. In a more recent study of $Al_3O_6H_2^-$, it was shown that three H_2O molecules would be added, which was consistent with a hexagonal structure calculated using DFT.[56] The DFT approach was used to differentiate the hexagonal structure from a double rhombus alternative, which was calculated to be slightly lower in energy.

Prior hydration experiments of larger aluminum oxide clusters have not been conducted, but the desire to examine systems that bore closer resemblance to alumina surfaces motivated ab initio calculations of hydration reactions of slightly larger clusters Al_4O_6 and Al_8O_{12}, which were chosen to mimic structural features on the Al terminated (0001) α-Al_2O_3 surface.[57] For Al_4O_6, dissociative adsorption was energetically preferred over molecular adsorption; however, the two processes were competitive in the case of Al_8O_{12}. In the latter case, dissociative 1−2 and 1−4 processes were examined, and the 1−4 process was found to be energetically more demanding than the 1−2; however, if a second H_2O were present, the 1−4 process was preferred, presumably due to a catalytic effect of

(29) Laiti, E.; Persson, P.; Ohman, L.-O. *Langmuir* **1998**, *14*, 825−831.
(30) Casey, W. H.; Phillips, B. L.; Karlsson, M.; Nordin, S.; Nordin, J. P.; Sullivan, D. J.; Neugebauer-Crawford, S. *Geochim. Cosmochim. Acta* **2000**, *64*, 2951−2964.
(31) Phillips, B. L.; Casey, W. H.; Karlsson, M. *Nature* **2000**, *404*, 379−382.
(32) Pak, M. V.; Gordon, M. S. *J. Chem. Phys.* **2003**, *118*, 4471−4476.
(33) Nemukhin, A. V.; Weinhold, F. *J. Chem. Phys.* **1992**, *97*, 3420−3430.
(34) Archibong, E. F.; St-Amant, A. *J. Phys. Chem A* **1999**, *103*, 109−1114.
(35) Chang, C.; Patzer, A. B. C.; Sedlmayr, E.; Sulzle, D. *Euro. Phys. J. D.* **1998**, *2*, 57−62.
(36) Patzer, A. B. C.; Chang, C.; Sedlmayr, E.; Sulzle, D. *Euro. Phys. J. D.* **1999**, *6*, 57−62.
(37) Archibong, E. F.; St-Amant, A. *J. Phys. Chem. A* **1998**, *102*, 6877−6882.
(38) Ghanty, T. K.; Davidson, R. R. *J. Phys. Chem. A* **1999**, *103*, 8985−8993.
(39) Akin, F. A.; Jarrold, C. C. *J. Chem. Phys.* **2003**, *113*, 1773−1778.
(40) Cui, X.-Y.; Morrison, I.; Han, J.-G. *J. Chem. Phys.* **2002**, *117*, 1077−1084.
(41) Martinez, A.; Tenorio, F. J.; Ortiz, J. V. *J. Phys. Chem. A* **2003**, *107*, 2589−2595.
(42) Martinez, A.; Tenorio, F. J.; Ortiz, J. V. *J. Phys. Chem. A* **2001**, *105*, 11291−11294.
(43) Chang, C.; Patzer, A. B. C.; Sedlmayr, E.; Steinke, T.; Sulzle, D. *Chem. Phys. Lett.* **2000**, *324*, 108−114.
(44) Rautta, S. A.; Hanley, L.; Anderson, S. L. *Chem. Phys. Lett.* **1987**, *137*, 5−9.
(45) Rautta, S. A.; Anderson, S. L. *J. Chem. Phys.* **1988**, *89*, 273−286.
(46) Jarrold, M. F. *J. Phys. Chem.* **1995**, *99*, 11−21.
(47) King, F. L.; Dunlap, B. I.; Parent, D. C. *J. Chem. Phys.* **1991**, *94*, 2578−2587.
(48) Cox, D. M.; Trevor, D. J.; Whetten, R. L.; Kaldor, A. *J. Phys. Chem.* **1988**, *92*, 421−429.
(49) Jarrold, M. F.; Bower, J. E. *J. Chem. Phys.* **1986**, *1986*, 5373−5375.
(50) Jarrold, M. F.; Bower, J. E. *J. Chem. Phys.* **1987**, *87*, 5728−5738.
(51) Jarrold, M. F.; Bower, J. E. *J. Am. Chem. Soc.* **1988**, *110*, 6706−6716.
(52) Hongbin, W. F.; Li, X.; Wang, X.-B.; Ding, C.-F.; Wang, L.-S. *J. Chem. Phys.* **1998**, *109*, 449−458.
(53) King, F. L.; Ross, M. M. In *Secondary Ion Mass Spectrometry SIMS VII*; Benninghoven, A., Evans, C. A., McKeegan, K. D., Storms, H. A., Werner, H. W., Eds.; John Wiley & Sons: Chichester, 1990; pp 53−56.
(54) Akin, F. A.; Jarrold, C. C. *J. Chem. Phys.* **2003**, *118*, 5841−5851.
(55) Scott, J. R.; Groenewold, G. S.; Gianotto, A. K.; Benson, M. T.; Wright, J. B. *J. Phys. Chem. A* **2000**, *104*, 7079−7090.
(56) Gowtham, S.; Lau, K. C.; Deshpande, M.; Pandey, R.; Gianotto, A. K.; Groenewold, G. S. *J. Phys. Chem. A* **2004**, in press.
(57) Wittbrodt, J. M.; Hase, W. L.; Schlegel, H. B. *J. Phys. Chem. B* **1998**, *102*, 6539−6548.

the second H_2O molecule. Other ab initio calculations revealed barriers to H_2O addition to alumina surfaces, which indicated that a comparable 1−4 addition should be substantially faster than the competing 1−2 process.[58] These studies compelled experimental investigations of larger, more extensively oxidized Al systems in order to relate cluster size and composition to hydrolysis reactivity.

In the present study, we have extended experimental hydration studies to fully oxidized alumina clusters containing up to 10 Al atoms. The clusters were produced by bombardment of gibbsite ($Al(OH)_3$) with an energetic polyatomic projectile that augments the production of larger cluster ions.[59−67] The combination of surface bombardment with a quadrupole ion trap secondary ion mass spectrometer (IT-SIMS)[68−71] has been used for the production and trapping of small ionic oxides and enabled reactivity studies of oxyanions of Al,[55,56] Si,[72,73] and Cr,[74,75] and oxycations of U.[76] The IT-SIMS has also been used for the production of larger aluminosilicate anions.[67] The extension of this capability to the generation of intermediately sized alumina cluster anions has provided the experimental basis for study of their hydration behavior.

Experimental Section

IT-SIMS: Vacuum Atmosphere. The IT-SIMS gas-phase atmosphere was strictly monitored by a Standard Bayard−Alpert Type (Varian, Lexington, MA) ion gauge calibrated against a Granville Phillips Stabil Ion Gauge (Boulder, CO). An additional pressure calibration was performed using an MKS Baratron absolute pressure transducer (Andover, MA). All three pressure measurement devices were mounted on the vacuum manifold. Additionally, an Inficon H200M residual gas analyzer (Inficon, Syracuse, NY) was mounted on the vacuum manifold to assess reliability of the relative ratios of the residual gases in the vacuum system. The IT-SIMS base pressure was typically 0.8×10^{-7} to 1.2×10^{-7} Torr and primarily consisted of H_2O, although substantial O_2, N_2, He, and H_2 were also present. A variable leak valve was used to control the partial pressure of H_2O vapor that had been admitted to the IT-SIMS prior to the ion−molecule reaction experiments. The H_2O pressure was maintained $(3.0-3.4) \times 10^{-7}$ Torr. Experiments conducted at H_2O pressures $< 3 \times 10^{-7}$ Torr would have been desirable; however we found that H_2O concentration could not be reliably measured below this value (which is also why multiple pressure measurement devices were employed). The pressure of He was maintained at 2×10^{-5} Torr. Our ion gauge response for H_2O was significantly different from the N_2 response,[77] thus ion gauge pressures were used to calculate H_2O number densities using a correction factor for ion gauge sensitivities derived from ion gauge calibration versus the capacitance manometer. The actual pressure within the ion trap itself could not be measured directly but is probably very close to that in the manifold.[55]

The gas-phase $Al_aO_{2a}H_{a-1}(H_2O)_w^-$ ions were produced from powdered synthetically prepared $Al(OH)_3$. The X-ray diffraction analyses confirmed that the prepared sample was predominantly gibbsite with a minor amount of bayerite (both $Al(OH)_3$ phases). $Al(OH)_3$ was attached to the end of a 2.7 mm probe tip using double-sided adhesive (3M, St. Paul, MN). The sputtered $Al_aO_{2a}H_{a-1}(H_2O)_w^-$ ions were trapped in the IT-SIMS, where they were subsequently reacted with the gaseous H_2O.

IT-SIMS: Ion−Molecule Reactions. The IT-SIMS was based on a modified Varian Saturn 2000 ITMS (Walnut Creek, CA)[68−71] equipped with a ReO_4^- primary ion gun[78−81] mounted collinear with the axis of the ion trap. The beam enters the ion trap through an aperture in the top end cap, passes along the main axis of the ion trap, and strikes the sample located behind the opposite end cap. The ReO_4^- ion gun was operated at 7.0 keV, at a primary ion current of ∼1200 pA measured using a Faraday cup.

The ReO_4^- beam was gated to only impact the sample during the ionization period of the IT-SIMS analysis sequence. Ionization times were adjusted to produce sufficient secondary ions to conduct the reactivity studies at an acceptable signal-to-noise level. The typical ionization time for the alumina/water reactivity studies was on the order of 0.1−0.2 s. Secondary ions sputtered from the sample surface were focused into the ion trap using a small cylindrical electrostatic lens, which also served to mitigate charge buildup on the bombarded sample surface.[82] During the ionization period, the alumina reactant ions of interest were isolated using selected ion storage,[83] which resulted in ejection of unwanted ions on the basis of their mass-dependent motional frequencies. Ion kinetic energies were standardized to the best of our ability by adjusting the trapping q_z value[83] to 0.7 for each ion isolated. Isolation of the dehydrated species was very difficult because of very fast reaction rates and fixed electronics settle times between ionization and scan-out; therefore the first or second hydrate ($w = 1, 2$; see Table 1) was normally isolated. Collision induced dissociation (CID) of the isolated ion produced a sufficient amount of the adjacent dehydrated ion to enable isolation and reliable measurement of hydration kinetics (although this approach did not work for the most dehydrated ions). Reaction times were varied systematically between ∼0.01 s and 10 s, and a q_z of 0.7 was also held throughout the reaction step. Finally, the ionic reactants and products were scanned out of the trap[83] and deflected

(58) Hass, K. C.; Schneider, W. F.; Curioni, A.; Andreoni, W. *Science* **1998**, *282*, 265−268.
(59) Appelhans, A. D.; Delmore, J. E. *Anal. Chem.* **1989**, *61*, 1087−1093.
(60) Hand, O. W.; Majumdar, T. K.; Cooks, R. G. *Int. J. Mass Spectrom. Ion Processes* **1990**, *97*, 35−45.
(61) Van Stipdonk, M. J.; English, R. D.; Schweikert, E. A. *Anal. Chem.* **2000**, *72*, 2618−2626.
(62) Van Stipdonk, M. J.; Justes, D. R.; Force, C. M.; Schweikert, E. A. *Anal. Chem.* **2000**, *72*, 2468−2474.
(63) Van Stipdonk, M. J.; Justes, D. R.; Santiago, V.; Schweikert, E. A. *Rapid Commun. Mass Spectrom.* **1998**, *12*, 1639−1643.
(64) Le Beyec, Y. *Int. J. Mass Spectrom. Ion Processes* **1998**, *174*, 101−117.
(65) Brunelle, A.; DellaNegra, S.; Deprun, C.; Depauw, J.; Hakansson, P.; Jacquet, D.; Le Beyec, Y.; Pautrat, M. *Int. J. Mass Spectrom. Ion Processes* **1997**, *164*, 193−200.
(66) Groenewold, G. S.; Delmore, J. E.; Olson, J. E.; Appelhans, A. D.; Ingram, J. C.; Dahl, D. A. *Int. J. Mass Spectrom. Ion Processes* **1997**, *163*, 185−195.
(67) Groenewold, G. S.; Kessinger, G. F.; Scott, J. R.; Gianotto, A. K.; Appelhans, A. D.; Delmore, J. E.; Avci, R. *Anal. Chem.* **2001**, *73*, 226−232.
(68) Groenewold, G. S.; Appelhans, A. D.; Ingram, J. C. *J. Am. Soc. Mass Spectrom.* **1998**, *9*, 35−41.
(69) Groenewold, G. S.; Appelhans, A. D.; Ingram, J. C.; Gresham, G. L.; Gianotto, A. K. *Talanta* **1998**, *47*, 981−986.
(70) Ingram, J. C.; Appelhans, A. D.; Groenewold, G. S. *Int. J. Mass Spectrom. Ion Processes* **1998**, *175*, 253−262.
(71) Gresham, G. L.; Groenewold, G. S.; Olson, J. E. *J. Mass Spectrom.* **2000**, *35*, 1460−1469.
(72) Groenewold, G. S.; Scott, J. R.; Gianotto, A. K.; Hodges, B. D. M.; Kessinger, G. F.; Benson, M. T.; Wright, J. B. *J. Phys. Chem. A* **2001**, *105*, 9681−9688.
(73) Groenewold, G. S.; Hodges, B. D. M.; Scott, J. R.; Gianotto, A. K.; Appelhans, A. D.; Kessinger, G. F.; Wright, J. B. *J. Phys. Chem. A* **2001**, *105*, 4059−4064.
(74) Gianotto, A. K.; Hodges, B. D. M.; Benson, M. T.; Harrington, P. d. B.; Appelhans, A. D.; Olson, J. E.; Groenewold, G. S. *J. Phys. Chem. A* **2003**, *107*, 5948−5955.
(75) Gianotto, A. K.; Hodges, B. D. M.; Harrington, P. B.; Appelhans, A. D.; Olson, J. E.; Groenewold, G. S. *J. Am. Soc. Mass Spectrom.* **2003**, *14*, 1067−1075.
(76) Gresham, G. L.; Gianotto, A. K.; Harrington, P. d. B.; Scott, J. R.; Olson, J. E.; Appelhans, A. D.; Groenewold, G. S. *J. Phys. Chem. A* **2003**, *107*, 8530−8538.
(77) Bartmess, J. E.; Georgiadis, R. M. *Vacuum* **1983**, *33*, 149−153.
(78) Delmore, J. E.; Appelhans, A. D.; Peterson, E. S. *Int. J. Mass Spectrom. Ion Processes* **1995**, *146/147*, 15−20.
(79) Delmore, J. E.; Appelhans, A. D.; Peterson, E. S. *Int. J. Mass Spectrom.* **1998**, *178*, 9−17.
(80) Delmore, J. E.; Appelhans, A. D.; Peterson, E. S. *Int. J. Mass Spectrom. Ion Processes* **1991**, *108*, 179−187.
(81) Johnson, K. B.; Delmore, J. E.; Appelhans, A. D. *Int. J. Mass Spectrom.* **2003**, *229*, 157−166.
(82) Dahl, D. A.; Appelhans, A. D. *Int. J. Mass Spectrom.* **1998**, *178*, 187−204.
(83) Todd, J. F. J., Ed. *Practical Aspects of Ion Trap Mass Spectrometry*; CRC Press: New York, 1995; Vol. 1.

Table 1. Compositions of $[Al_aO_{2a}H_{a-1}(H_2O)_w]^-$, Formed by Direct Sputtering of $Al(OH)_3$, CID, and Hydration Reactions

Masses of Cluster Ions $[Al_aO_{2a}H_{a-1}(H_2O)_w]$ Generated in the Ion Trap Secondary Ion Mass Spectrometer (IT-SIMS)								
	w							
a	−3	−2	1	0	+1	+2	+3	+4
1	n.a.[a]	n.a.	n.a.	59	77	95	n.o.[b]	n.o.
2	n.a.	n.a.	n.a.	119	137	155	173	n.o.
3	n.a.	n.a.	161[c]	179	197	215	233	n.o.
4	n.a.	n.a.	221[c]	239	257	275	293	n.o.
5	n.a.	263[c]	281[c]	299	317	335	n.o.	n.o.
6	n.a.	323[c]	341[c]	359	377	395	413	n.o.
7	365[c]	383[c]	401[c]	419	437	455	473	n.o.
8	425[d]	443[d]	461[c]	479	497	515	533	n.o.
9	485[d]	503[d]	521[d]	539	557	575	593	n.o.
10	545[d]	563[d]	581[d]	599[d]	617[d]	635[d]	>m.r.[e]	>m.r.

[a] The loss of water is not applicable. [b] The ion is not observed after a 1 s reaction time. [c] These ions are observed after CID. [d] The ion is observed in MS 1 spectra, but ion abundance is insufficient for isolation and water reactivity studies. [e] The mass of interest is greater than the mass range of the instrument.

onto a Venetian blind dynode positioned in front of the multichannel plate detector, located off axis between the end of the ion trap and the primary ion gun. Three spectra (each a sum of 30 microscans) were collected at each time interval, which enabled the variability in the relative abundances to be assessed at each time point.

Kinetic Analysis. Analyses of the kinetic data sets were completed using a commercially available software package (Berkeley Madonna),[84] which is a general purpose differential equation solver that utilizes a Runge−Kutta integration algorithm. Kinetic plots in agreement with the data could be generated using a model that included serial forward hydration reactions. Reverse reactions did not play a significant role in any of the kinetic schemes. The three IT-SIMS data sets were loaded individually, and rates were generated for the sequential hydration steps. Rate constants (k_1, k_2, k_3, k_4) were generated by dividing the individual rates by the H_2O number density, which ranged from 2.2×10^{10} to 2.3×10^{10} cm^3 mL c^{-1} s^{-1}. The three rate constants were then averaged and reported. The root-mean-square (rms) error was calculated to determine how accurately the modeled line generated from Berkeley Madonna fit the experimental data.

Reaction Efficiency. Reaction efficiency was evaluated by comparing forward rate constants from the fitted kinetic analyses with theoretical rate constants calculated using the reparametrized average-dipole-orientation (ADO) theory.[85−89] The reparametrized ADO constants were calculated using a reaction temperature (310 K), which was the average ion temperature for an ion in a typical trap as calculated by Goeringer and McLuckey[90] and Gronert.[91]

Results and Discussion

Secondary Ion Mass Spectrum of $Al(OH)_3$. Alumina cluster ions were generated by bombarding the surface of $Al(OH)_3$ with energetic projectiles. The mass spectrum of the resulting secondary ions (Figure 1) acquired using conditions where the ion lifetime was short (relative to ion trap parameters, e.g., 0.01−0.032 s) showed a series of cluster ions that corresponded

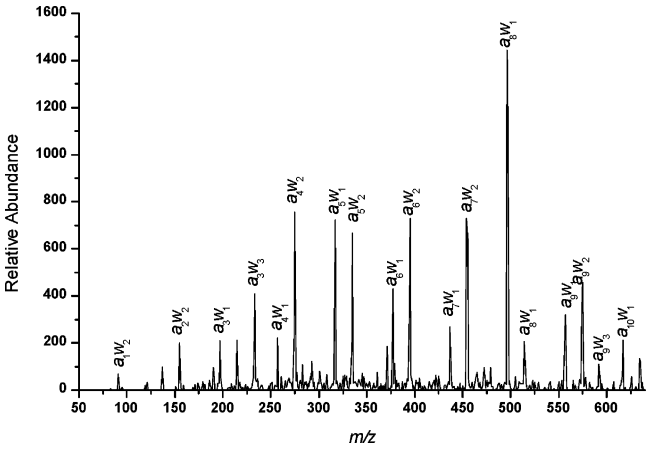

Figure 1. Mass spectrum of $Al(OH)_3$ acquired using the ion trap secondary ion mass spectrometer.

to the general formula $[Al_aO_{2a}H_{a1}(H_2O)_w]^-$, where *a* corresponds to the number of Al atoms, and *w* is the number of condensed water molecules attached to the cluster. For example, the prominent ion at *m*/*z* 497 corresponds to $a = 8$ and $w = 1$ (denoted *a*8*w*1); for *m*/*z* 275, $a = 4$, and $w = 2$ (*a*4*w*2).

Table 1 shows a summary of the cluster ions that were generated either by SIMS or SIMS plus CID (for low *w*). We emphasize that this approach to formula designation does not imply that H_2O is molecularly adsorbed to the cluster anions but easily conveys the extent of hydration relative to the most prominent ion series observed under low-pressure conditions. The spectrum is similar to that generated by Akin and Jarrold under water "saturated" conditions using laser ablation to produce clusters: abundant ions at *m*/*z* 155, 173, and 233 were recorded.[54] We observed that when the $Al(OH)_3$ solid remained in a vacuum for periods of 8 h or longer prior to analysis, the abundances of ions having $w > 0$ decreased and *w*0 ions appeared. Extended time in a vacuum tended to decrease the water vapor pressure and the adsorbed water on the $Al(OH)_3$ surface, which both foster hydrated species either during the sputtering event or as a result of ion−molecule reactions.

The appearance of alumina clusters from $1 \le a \le 10$ provided an opportunity to examine the extent of hydration and the reaction kinetics as cluster size increases. To accomplish this, clusters were isolated in the quadrupole ion trap under conditions where the water partial pressure was carefully controlled at a measurable value and where the kinetic energy of the ions was normalized to the greatest extent possible within our instrument. Both factors had a direct effect on the observed reaction rate. We empirically found that reliable rate constants could not be measured at $[H_2O] < \sim 3 \times 10^{-7}$ Torr (see Experimental Section); therefore, all rate constant measurements were made at $[H_2O] \ge 3 \times 10^{-7}$ Torr. Because the dehydrated ions underwent rapid hydration before scan-out could be initiated even under the shortest time scales (~0.01 to 0.035 s in these experiments), this precluded accurate measurement of the rate constants for most of the dehydrated ions ($w = -1, 0$). In some cases, it was possible to generate more dehydrated ions using collisional activation, but these ions immediately began hydrating as soon as they were formed. Consequently, we believe that these reactions are proceeding at or near the collision constant.

Control of ion kinetic energy was important for reactivity comparison, because the apparent rates of the ion−molecule

(84) Zahnley, T.; Macey, R.; Oster, G. *Berkeley Madonna*, 8.0.1 ed.; University of California: Berkeley, CA, 2003.
(85) Su, T.; Chesnavich, W. J. *J. Chem. Phys.* **1982**, *76*, 5183−5185.
(86) Su, T.; Bowers, M. T. *Int. J. Mass Spectrom. Ion Phys.* **1975**, *17*, 211−212.
(87) Su, T.; Bowers, M. T. *J. Am. Chem. Soc.* **1973**, *95*, 7609−7610.
(88) Su, T.; Bowers, M. T. *J. Am. Chem. Soc.* **1973**, *95*, 7611−7613.
(89) Su, T.; Bowers, M. T. *Int. J. Mass Spectrom. Ion Phys.* **1973**, *12*, 347−356.
(90) Goeringer, D. E.; McLuckey, S. A. *Int. J. Mass Spectrom. Ion Processes* **1998**, *177*, 163−174.
(91) Gronert, S. *J. Am. Soc. Mass Spectrom.* **1998**, *9*, 845−848.

Scheme 1. Hydration of *a*3*w*1 ($[Al_3O_6H_2(H_2O)]^-$), Showing the Formation of the Activated Complex, Followed by Either Reversion to Reactants or Stabilization to Form Products

$$[Al_3O_6H_2(H_2O)_1]^- + H_2O \rightleftharpoons [Al_3O_6H_2(H_2O)_2]^{-*}$$

$$[Al_3O_6H_2(H_2O)_2]^{-*} \xrightarrow{He} [Al_3O_6H_2(H_2O)_2]^-$$

reactions were strongly influenced by this factor. The dependence is a consequence of the fact that the reactions were ternary,[92,93] with the rates being dependent on both H_2O and He concentration. The reverse reaction depicted in Scheme 1 was strongly dependent on the energy of the activated complex, which is largely derived from the kinetic energy of the reactants. When the kinetic energy of the reactant ion is high, the formation of the stable hydrate is slowed or even precluded by rapid reversion of the activated complex to reactants.[94] This behavior was confirmed by resonantly exciting alumina clusters, which resulted in cessation of formation of the next stable hydrate. In an attempt to normalize the average kinetic energy of the ions in the trap, we adopted a protocol in which all reactant ions were isolated at a q_z value of 0.7; kinetic modeling of these experiments indicated that back reactions were negligible at this q_z value.

Before discussing hydration behavior of individual clusters, it is worthwhile noting that the clusters produced are fully oxidized, that is, not reactive with O_2. For example, oxidation experiments were attempted with the *a*3*w*1 species by increasing the experimental partial pressures of O_2 to 3×10^{-6} Torr.

The *a*3*w*1 series of ions did not oxidize under our experimental parameters. Hence no further research was conducted with O_2.

***a*2 Clusters.** Previous experiments in which $[Al_2O_4H]^-$ (*a*2*w*0, *m*/*z* 119) was isolated and reacted with water showed that the molecule would rapidly add two H_2O molecules in a dissociative fashion to produce *a*2*w*1 and *a*2*w*2 at *m*/*z* 137 and 155, respectively (Figures 2 and 3, Scheme 2).[55] We repeated those experiments using a newer version IT-SIMS that has improved trapping efficiency of low abundance product ions over longer time periods. This revealed a slow addition of a third H_2O to form *a*2*w*3 at *m*/*z* 173. The kinetic profile of the *a*2 reactant and product ions was consistent with three serial reactions (Figure 3), for which rate constants were calculated[84] (Table 2). The rate for addition of the third H_2O was substantially slower (4% eff.) compared to the rates for addition of the first and second H_2O molecules, which proceeded at the collision constant.

Previous ab initio calculations of the *a*2 clusters showed a minimum energy structure for $Al_2O_4H^-$ that contained an Al_2O_2 rhombus with O atoms pendant on the Al atoms.[33,37,55] Dissociative addition of one and two H_2O molecules did not disrupt the Al_2O_2 rhombus.[55] If the rhombic structure is what we have in the present experiments, then the addition of the third H_2O molecule poses an interesting structural problem, because the tetrahedral Al atoms in *a*2*w*2 at *m*/*z* 155 can no longer function as Lewis acids. Dissociative addition of the third water should not occur unless a Lewis acid site is somehow induced, which could occur if the rhombus was ruptured, leading to an acyclic

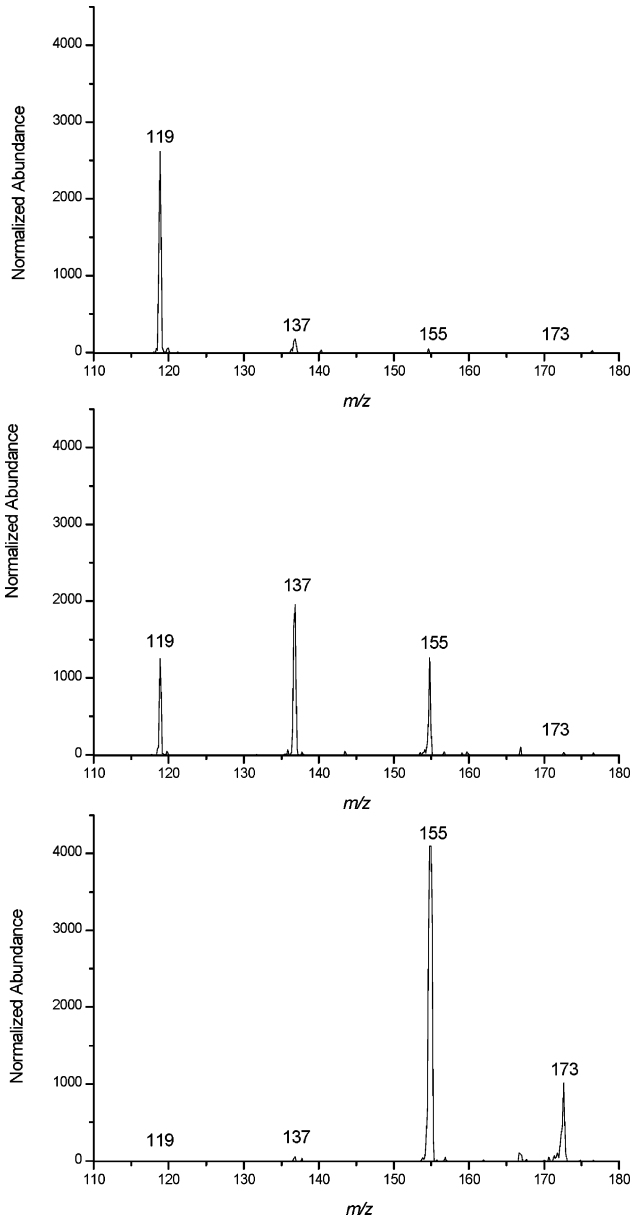

Figure 2. Mass spectra of *a*2*w*0 formed by isolation and CID of *m*/*z* 155 *a*2*w*2 in $\leq 3 \times 10^{-7}$ Torr H_2O followed by periodic mass analysis at variable reaction times. The delay times for the three mass spectra are 0.010 s (top), 0.069 s (middle), and 1.012 s (bottom).

structure (*a*2*w*3). Such a process might be spurred by the presence of a bridging hydroxyl, which compared with a bridging oxo would decrease electron density around the Al centers, facilitating attack by another H_2O; this explanation would be consistent with the studies of Casey and co-workers, who showed that bridging hydroxyls on Keggin-like complexes were exchangeable on an NMR time scale.[30,31] Such a process would be expected to have a very constrained mechanism that would be consistent with the low reaction efficiency. An alternative explanation for the addition of the third H_2O would be formation of a hydrogen bound structure; however, we do not favor this because loosely bound adducts tend not to be observed in the IT-SIMS; for example, alkali$^+$(H_2O) adducts[95] are not observed, which would be expected to have bond

(92) Gilbert, R. G.; Smith, S. C. *Theory of Unimolecular and Recombination Reactions*; 1st ed.; Blackwell Scientific Publications: London, 1990.
(93) Weishaar, J. C. *Acc. Chem. Res.* **1993**, *26*, 213−219.
(94) Jackson, G. P.; Gibson, J. K.; Duckworth, D. C. *Int. J. Mass Spectrom.* **2002**, *220*, 419−441.
(95) Rodgers, M. T.; Armentrout, P. B. *Mass Spectrom. Rev.* **2000**, *19*, 215−247.

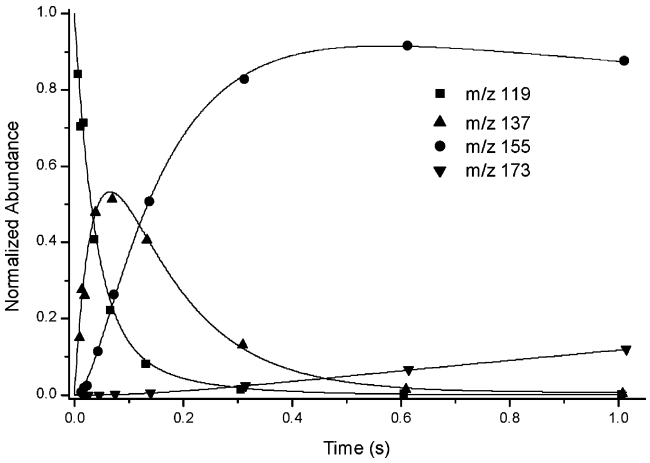

Figure 3. Kinetic plot of *a*2*w*0 isolated in $\leq 3 \times 10^{-7}$ Torr H_2O. The points represent data from an experimental set, and the lines were generated from the kinetic model.

Scheme 2. Hydration Reactions for $[Al_2O_4H]^-$ [a]

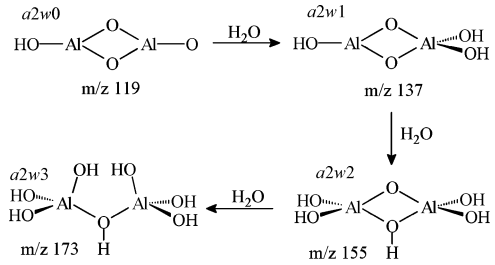

[a] Structures for *a*2*w*0, *a*2*w*1, and *a*2*w*2 are schematic representations of those calculated using ab initio approaches; the structure for *a*2*w*3 has not yet been calculated and is speculative, based on proposed dissociative addition of the third H_2O, which involves rupture of the Al_2O_2 rhombus.

energies comparable to those of hydroxide(H_2O) adducts,[96] which would serve as a model for what might be formed in the present case. There was no evidence for the addition of a fourth H_2O in these experiments. Within any of the a_n ion envelopes, there is the possibility of multiple ion structures that are energetically competitive. For the a_2 systems, we believe multiple structures are less likely because the DFT calculations[55] did not indicate the presence of competitive isomers. However, for $a \geq 3$, the existence of multiple isomers becomes more probable, opening up the possibility of a variable number of reactive sites for the ensemble of ions at a given mass.

***a*3 Clusters.** Ions corresponding to *a*3*w*0 (*m*/*z* 179) could be isolated only with difficulty at low water pressures, and for this reason, reactivity studies were conducted by isolating *a*3*w*1 (*m*/*z* 197). Starting from this point, CID was used to generate *a*3*w*0 and *a*3*w*−1 ($Al_3O_6H_2^-$ and $Al_3O_5^-$ at *m*/*z* 161 and 179, respectively) (Figures 4 and 5). Rehydration of these ions in a pressure regime where H_2O concentration was accurately known ($> 3 \times 10^{-7}$ Torr) was effectively immediate, which meant that data for rate modeling had to come from the tail of the exponential decay and the resulting rates were imprecise. When the H_2O concentration was decreased, better decay data was produced, but the measured rate constants exceeded the ADO collision constant by up to a factor of 2. This suggested that at low pressures H_2O concentration was actually somewhat higher than what was being recorded by the ion gauges, reflecting

Table 2. Hydration Rate Constants for $[Al_aO_{2a}H_{a-1}(H_2O)_w]^-$

a	*w* → *w* + 1	*k*[a]	eff[b] (%)	rms error[c]
2	0 → 1	c.c[d]	100	
2	1 → 2	2.2×10^{-9} [e]	100	0.010
2	2 → 3	8.6×10^{-11}	4	0.024
2	3 → 4	$\leq 1 \times 10^{-12}$ [f]	≤0.05	0.018
3	−1 → 0	c.c	100	
3	0 → 1	c.c	100	
3	1 → 2	1.6×10^{-9}	76	0.020
3	2 → 3	2.2×10^{-9}	100	0.020
3	3 → 4	$\leq 1 \times 10^{-12}$[f]	≤0.05	0.023
4	0 → 1	c.c	100	
4	1 → 2	2.2×10^{-9}[e]	100	0.030
4	2 → 3	4.0×10^{-10}	19	0.053
4	3 → 4	$\leq 1 \times 10^{-11}$[f]	≤0.48	0.040
5	0 → 1	c.c	100	
5	1 → 2	6.8×10^{-10}	28	0.042
5	2 → 3	$\leq 1 \times 10^{-12}$[g]	≤0.05	0.033
6	0 → 1	c.c	100	
6	1 → 2	6.5×10^{-10}	30	0.12
6	2 → 3	6.0×10^{-12}	0.28	0.10
6	3 → 4	$\leq 7 \times 10^{-12}$[g]	≤0.33	0.025
7	0 → 1	c.c	100	
7	1 → 2	1.9×10^{-9}	87	0.034
7	2 → 3	3.4×10^{-11}	2	0.027
7	3 → 4	$\leq 1 \times 10^{-12}$[g]	≤0.05	0.0074
8	0 → 1	c.c	100	
8	1 → 2	8.8×10^{-11}	4	0.17
8	2 → 3	9.6×10^{-11}	5	0.10
8	3 → 4	$\leq 1 \times 10^{-12}$[g]	≤0.05	0.15
9	0 → 1	c.c	100	
9	1 → 2	8.3×10^{-10}	39	0.025
9	2 → 3	2.9×10^{-10}	14	0.038
9	3 → 4	$\leq 1 \times 10^{-12}$[g]	≤0.05	0.027

[a] Average rate constant reported in cm^3 mL c^{-1} s^{-1}. [b] Average efficiency as a percentage of ADO. [c] Root-mean-square error (a measure of the accuracy of the modeled line versus experimental data). [d] Rate occurring at ADO collision constant, which ranged from 2.1×10^{-9} to 2.2×10^{-9}. [e] The experimental value recorded higher, although we believe associated with error of measurement. The theoretical rate constant is reported. [f] Estimated rate constant if addition of water was to occur; i.e. specie would be present at 10 counts at a 0.3 s reaction time. [g] Estimated rate constant if addition of water was to occur; i.e. specie would be present at 10 counts at a 1 s reaction time.

difficulty in measuring H_2O concentration at values low enough to perform accurate determinations of rate constants (see Experimental Section). In these instances, the rate constants were reported as the collision constant (Table 2). For the *a*3 clusters, hydration rate constants or $w = -1 \rightarrow 0$, $0 \rightarrow 1$, $1 \rightarrow 2$, and $2 \rightarrow 3$ were at or near the ADO collision constant. After addition of the third H_2O, the hydration sequence comes to an abrupt halt: there was no evidence for addition of a fourth H_2O up to a 1 s reaction time.

Using DFT calculations, the ultimate product (*a*3*w*3) was interpreted in terms of the trihydrate having a hexagonal Al_3O_3 structure (Scheme 3), with two pendant O atoms on each (tetrahedral) Al atom.[40,56] This *a*3*w*3 structure would have no trigonal Al atoms that would function as Lewis acid sites, and hence would be resistant to further hydrolysis reactions. We believe that the hexagonal structure for *a*3*w*3 is very easily reconciled with the bent windowpane structure calculated for *a*3*w*−1 ($Al_3O_5^-$) by Ortiz and co-workers (Scheme 3,[42] attack on the central Al atom as proposed by Akin and Jarrold[54]), which could rupture the central Al−O bond, forming a hexagonal

(96) Merrill, G. N.; Webb, S. P. *J. Phys. Chem. A* **2003**, *107*, 7852−7860.

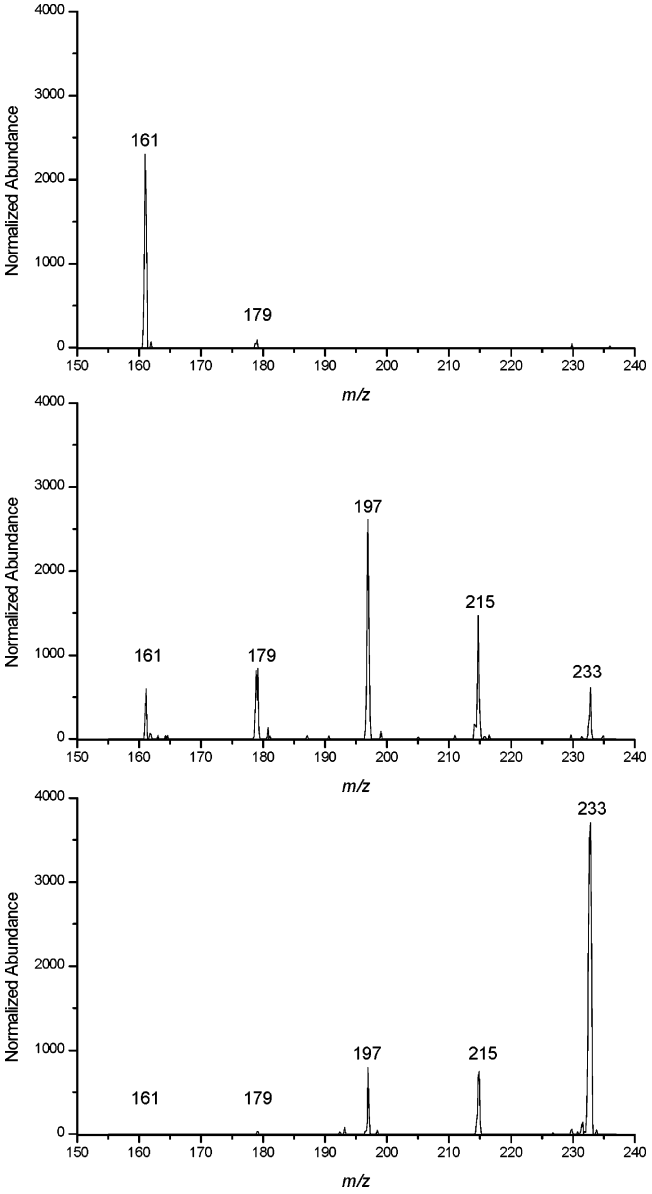

Figure 4. Mass spectra of *a*3*w*−1 formed by isolation and CID of *m*/*z* 179 in an IT-SIMS at ≤3 × 10^{-7} Torr H_2O. The delay times for the three mass spectra are 0.011 s (top), 0.032 s (middle), and 1.02 s (bottom).

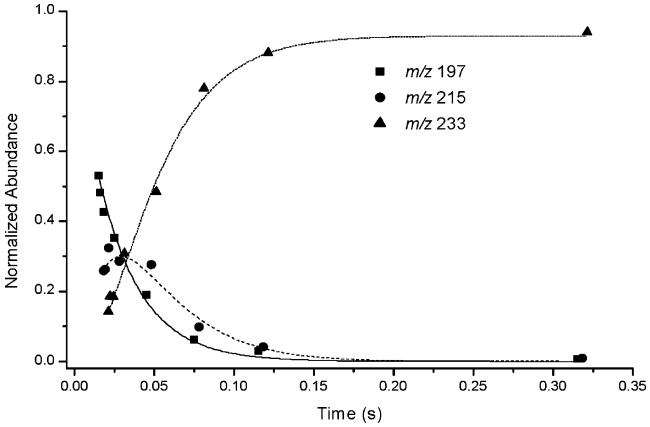

Figure 5. Kinetic plot of *a*3*w*1 isolated in 3 × 10^{-7} Torr H_2O. The points represent data from an experimental set, and the lines were generated from the kinetic model.

Scheme 3. Schematic Representation of Structure for *a*3*w*−1, Based on the Calculations by Ortiz[42] [a]

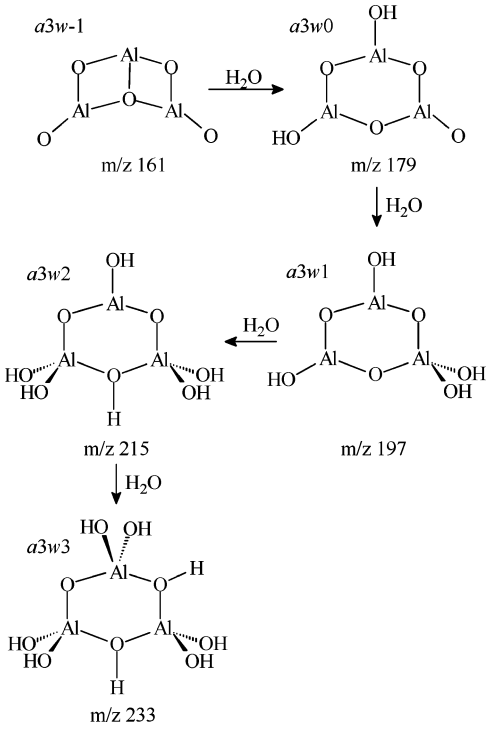

[a] Schematic representation of structures for *a*3*w*0, *a*3*w*1, *a*3*w*2, and *a*3*w*3 are based on the mode of attack proposed by Akin and Jarrold[54] and the structure proposed for the Al_3O_6 anion by Gowtham.[56]

structure with one additional undercoordinated Al atom that would be susceptible to hydrolysis.

***a*4−*a*10 Clusters.** The number of structural possibilities and commensurate variations in reactivity begin to increase rapidly when clusters for which $a > 3$ are considered.[40,56] Nevertheless, the hydration reactions provide insight into the number of reactive sites on the clusters. Ions for which $a = 4$ and $w = 0$ (*m*/*z* 239) were not easily isolated at a water pressure of >3 × 10^{-7} Torr. The $0 \rightarrow 1$ rate constant could not be measured, as the dehydrated reactant had already added the first water under these conditions. Experiments conducted at lower H_2O concentration in fact confirmed the reaction pathway, but uncertainties in the H_2O concentration prevented accurate rates from being determined. To this end, reactivity studies were conducted by isolating *a*4*w*2 (*m*/*z* 275) and then generating *a*4*w*1 using CID (spectra and kinetic plots are provided in Supporting Information). The rate constants for the *a*4 clusters were at the ADO collision constant for $w = 0 \rightarrow 1$ and $1 \rightarrow 2$; however, $2 \rightarrow 3$ was slower by a factor of 5, and $3 \rightarrow 4$ did not occur at all. Based on conclusions from the *a*2 and *a*3 systems, this suggested that the *a*4*w*0 ion contained three trigonally coordinated Lewis acid Al sites or perhaps two sites plus one site that can be induced by one of the hydration steps. A bicyclic structure with two rings would satisfy these criteria because that would necessitate three trigonal Al sites. An alternative explanation would be an adamantyl-type structure that contains one hydroxyl bridge: this is an attractive suggestion because it would contain two trigonal Al sites susceptible to rapid hydrolysis and one hydroxyl bridge capable of inducing slow hydrolysis at a vicinal Al. Furthermore it would be consistent with the slow isotopic oxygen exchange observed for bridging hydroxyls in solution aluminum oxide complexes.[30,31] The open, hexagonal structures

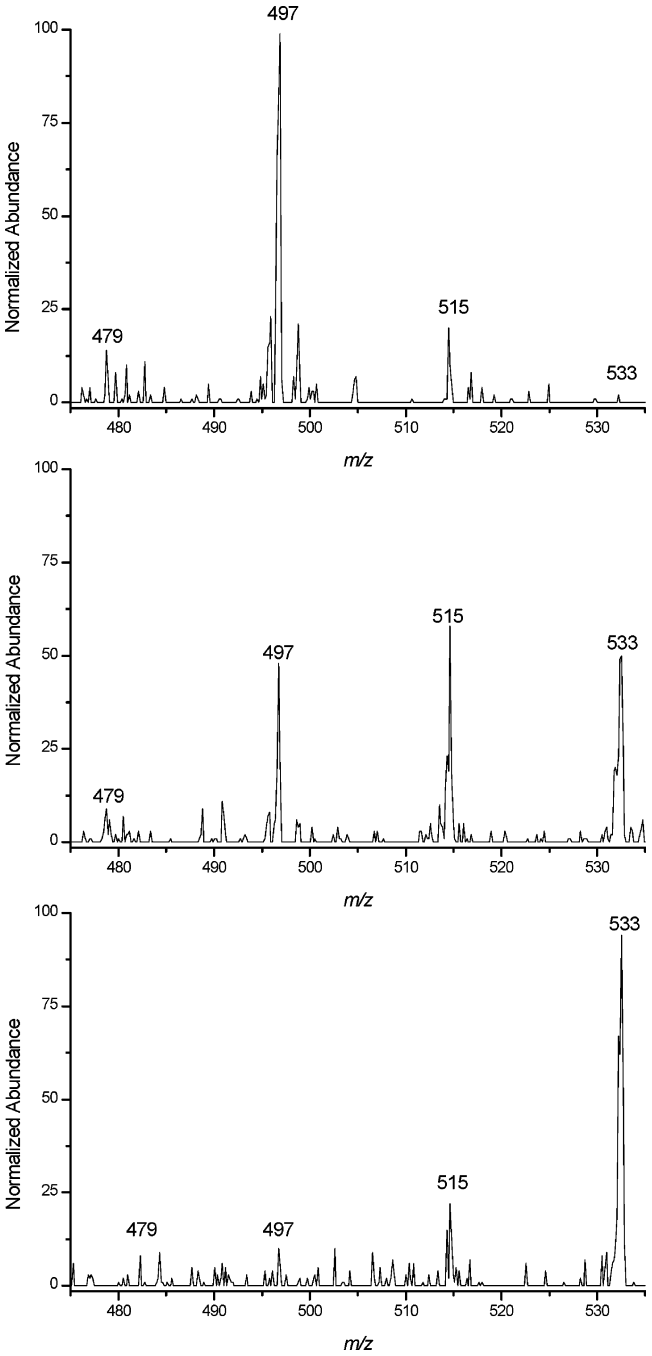

Figure 6. Mass spectra of *a*8 clusters $[Al_8O_{16}H_7(H_2O)_w]^-$ formed by isolation of *a*8*w*1 (*m*/*z* 497) in 3×10^{-7} Torr H_2O followed by periodic mass analysis after 0.02 s (top), 1.02 s (middle), and 10.03 s (bottom).

have not been computationally examined; however, the structure would be consistent with the trend toward stable, hexagonal ring structures that was noted in the recent DFT study of *a*3 systems.[56] Clearly there are other structures that would satisfy the constraints established by the hydration reactivity study, and in fact, multiple structures that are energetically competitive would be expected. Interestingly, a structure for *a*4*w*0 containing a cubic T_d Al_4O_4 moiety[43] with pendant O atoms off the Al centers would not be expected to be at all reactive with H_2O, since all Al centers in this structure would be tetravalent.

The *w*0 clusters of *a*5 through *a*9 all added an initial H_2O at the collision constant, which, as in the case of the *a*2 through *a*4 clusters, suggested the presence of a trigonal Al center in

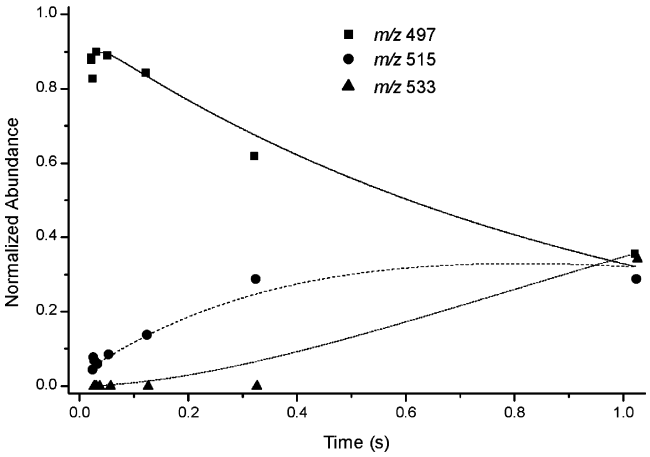

Figure 7. Kinetic plot of *a*8*w*1 isolated in 3×10^{-7} Torr water. The points represent data from an experimental set, and the lines were generated from the kinetic model.

each of these ions. Data for the *a*8 clusters is typical (Figures 6 and 7), and data for the *a*5, *a*6, *a*7, and *a*9 systems are provided in the Supporting Information. More size-distinctive behavior was observed starting with the addition of the second H_2O. Formation of *w*2 was very fast for *a*7 (87% efficient) and also substantial for *a*5, *a*6, and *a*9 (efficiencies ranging from 28% to 39%). The reactivity of *a*8 was in sharp contrast, however, with an efficiency of only 4%, which indicates that the second reactive site on this molecule is significantly more hindered, perhaps a tetrahedral Al adjacent to a bridging OH.

Variations in reactivity are also pronounced relative to the addition of a third H_2O. The *a*5 cluster was unreactive relative to addition of a third H_2O, which was surprising, since this occurred readily for both *a*3 and *a*4. But beyond $a = 5$, k_3 values increased steadily with increasing *a*. A priori, this is what was expected: increasing hydration reactivity reflecting additional reactive sites as the size of the clusters increased. However, addition of a fourth H_2O was not observed in any of the clusters up to a 1 s reaction time.

We note in passing that clusters corresponding to *a*10*w*1 and *a*10*w*2 were also observed in the mass spectrum of $Al(OH)_3$, indicating that at least two H_2O molecules will add to the *a*10*w*0 cluster; whether a third H_2O will add is unknown because the mass of *a*10*w*3 was beyond the mass range of the IT-SIMS (635 u). The kinetics of this system was not pursued because ion isolation this close to the upper mass limit was inefficient.

Generalizing, the results of the reactivity studies showed that the extent of hydration stopped at three H_2O molecules for $Al_aO_{2a}H_{a-1}^-$ clusters, for values of *a* ranging from 2 through 9. The fact that the extent of hydration did not increase regularly with increasing *a* indicated that the structure of the clusters was becoming more condensed. That is, the number of bridging oxo- and hydroxyl-moieties increases as the structures incorporate a larger number of rings; conversely stated, the number of reactive trigonal centers per Al atom is decreasing. The relative rates for addition of three H_2O molecules that were observed in the $a = 2$ cluster, viz. fast addition of the initial two H_2O molecules followed by a slow addition of a third H_2O, constitutes a theme that is repeated for $a = 4$, 6, 7, and 9. The explanation for the $a = 2$ cluster, in which the addition of the first two H_2O molecules involved efficient attack on a trigonal Lewis acid Al center and addition of the third involved a much slower attack

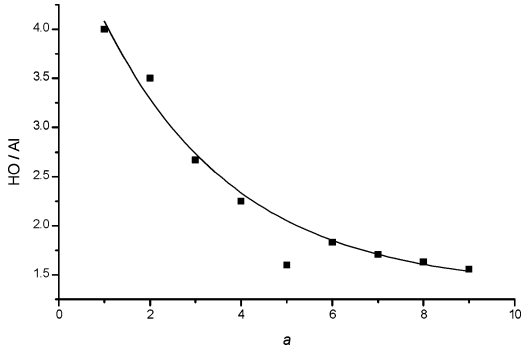

Figure 8. Ratio of hydroxyls to Al atoms (OH/Al) versus cluster size *a*. Data are represented by the squares, and the line represents a fitted exponential decay. The HO/Al ratio for $a = 1$ was reported in ref 55. The HO/Al value for $a = 5$ was clearly an outlier and not used in the modeling exercise.

on an Al vicinal to a hydroxyl bridge, may be extendable to the larger clusters and would constitute a good starting point for computational investigations. The *a*3, *a*5, and *a*8 clusters do not strongly adhere to this trend; *a*3 is highly reactive with three H_2O molecules, whereas, in contrast, *a*5 adds only two, and *a*8 quickly adds only one. These findings clearly signal significant alterations in the structure and consequent reactivity of the clusters.

The hydroxyl coverage of the largest aluminum oxide cluster of the present study is reasonably comparable to that expected for alumina surfaces. The ratio HO/Al was calculated for the maximum *w* value observed for clusters at each *a* value, assuming that all H_2O molecules were dissociatively added. The HO/Al was then plotted versus *a* (Figure 8) and was modeled using an exponential decay. This suggested that, for values of $a > 13$, a relatively constant HO/Al ratio of $\sim$1.3−1.4 could be expected. This is moderately higher than the value of $\sim$1.0 reported for α-Al_2O_3(0001) by Elam and co-workers;[97] however, they noted that other forms of alumina react more readily with H_2O and, hence, may have higher saturation hydroxyl coverage, perhaps in closer agreement with the model for the gas-phase clusters $a > 13$.

Conclusion

These investigations set the stage for reactivity studies of the alumina clusters that have the potential for close resemblance to hydroxylated surfaces. Since the role of the hydroxyl groups is not well understood,[97] the experiments may provide an augmented level of insight: in particular, they are indicative of the number and also suggestive of the types of reactive sites. Clearly, the larger clusters will challenge structural calculations; nevertheless, the ability to experimentally identify the number of reactive sites could provide a useful validation approach for computational results generated for larger metal oxide systems.

Acknowledgment. The United States Department of Energy Environmental Systems Research Program under Contract DE-AC-07-99ID13727 BBWI supported this research. The authors are indebted to Dr. David Cummings for the synthesis of the gibbsite $Al(OH)_3$.

Supporting Information Available: Spectra and kinetic plots are available for *a*4*w*1 through *a*9*w*1 excluding *a*8*w*1. This material is available free of charge via the Internet at http://pubs.acs.org.

JA0492945

(97) Elam, J. W.; Nelson, C. E.; Cameron, M. A.; Tolbert, M. A.; George, S. M. *J. Phys. Chem. B* **1998**, *102*, 7008−7015.